ISSN 1063-7826, Semiconductors, 2020, Vol. 54, No. 8, pp. 869–876. © Pleiades Publishing, Ltd., 2020.
Russian Text © The Author(s), 2020, published in Fizika i Tekhnika Poluprovodnikov, 2020, Vol. 54, No. 8, pp. 721–728.

PHYSICS OF SEMICONDUCTOR DEVICES

On the Current Dependence of the Injection Efficiency and the Relative Contribution of the Escape Rate and Internal Optical Loss to Saturation of the Power–Current Characteristics of High-Power Pulsed Lasers ($\lambda = 1.06$ μm)

A. V. Rozhkov*

Ioffe Institute, St. Petersburg, 194021 Russia

**e-mail: rozh@hv.ioffe.rssi.ru*

Received March 5, 2020; revised March 23, 2020; accepted March 23, 2020

Abstract—The results of numerical simulation of the current dependence of the efficiency of injection into the active area of a laser based on separate-confinement double heterostructures are reported. The feature of carrier transport through isotype *N–n* heterojunctions at the interface between the waveguide and active areas is demonstrated. Using the classic dependences of the Drude–Lorentz theory, the electron (σ_e) and hole (σ_p) scattering cross sections for a GaAs waveguide are estimated. Using the obtained values of $\sigma_e = 1.05 \times 10^{-18}$ cm^2 and $\sigma_p = 1.55 \times 10^{-19}$ cm^2 and the current dependences of the injection efficiency, the primary cause for confinement of the pulse power of the semiconductor lasers is determined. It is established that the internal optical loss is a minor fraction of the loss and the decisive contribution to saturation of the power–current (*P–I*) characteristics is made by the escape of holes to the waveguide.

Keywords: thermionic emission, semiconductor laser, isotype heterojunction, saturation of the *P–I* characteristic

DOI: 10.1134/S1063782620080217

1. INTRODUCTION

A review of numerous studies on saturation of the pulsed power of lasers based on separate-confinement double heterostructures (SCDHs) reveals the need for refining some key parameters and performing an additional numerical analysis in order to establish the role of the internal optical loss and the rate of carrier escape from the quantum-confined active region.

In recent years, in studying the current-efficiency saturation in high-power semiconductor lasers, several models taking into account different mechanisms affecting the optical power loss in a laser cavity have been proposed and investigated. The cross sections of scattering of mobile carriers (electrons (σ_e and holes σ_p) are the key parameters of each of the proposed models. Unfortunately, the direct experimental methods used for measuring the effect of free carriers are complex, while calculated relations are either lacking or unclear. Therefore, it is impossible to determine the relative contribution of the internal optical loss because of a significant difference in the reported σ_e and σ_p values. Among a great list of studies, we should note the following examples, including the investigated mechanisms and the σ_e and σ_p values used: free carrier absorption (FCA), $\sigma_e = 3 \times 10^{-18}$ cm^2 and $\sigma_p = 7 \times 10^{-18}$ cm^2 [1]; FCA with regard to the longitudinal spatial nonuniformity of the density distribution and longitudinal spatial hole burning (LSHB) *G* in a cavity, $\sigma_e = 4 \times 10^{-18}$ cm^2 and $\sigma_p = 12 \times 10^{-18}$ cm^2, $\sigma_e = 4 \times 10^{-30}$ cm^2 and $\sigma_p = 12 \times 10^{-30}$ cm^2 in [2, 3], respectively; and FCA taking into account two-photon absorption (TPA) with subsequent free-carrier density redistribution (the secondary FCA effect, TPA-generated carriers (FCA TPA)) $\sigma_e = 3 \times 10^{-18}$ cm^2 and $\sigma_p = 1 \times 10^{-17}$ cm^2, $\sigma_e = 5 \times 10^{-19}$ cm^2 and $\sigma_p = 4 \times 10^{-17}$ cm^2 [4, 5], respectively. Nevertheless, the authors of [6, 7] analyzed the results of a one- and two-dimensional simulation for values of $\sigma_e = 4 \times 10^{-18}$ cm^2 and $\sigma_p = 12 \times 10^{-18}$ cm^2 and determined the relative contributions of the two main mechanisms, FCA and spontaneous recombination in the waveguide regions, due to the leakage of carriers from the quantum well (QW), which is called the carrier-leakage effect. Uncertainty in the σ_e and σ_p values used was mentioned also in other studies on the efficiency of high-power pulsed lasers.

The much weaker interest in studying the efficiency of injection into the QWs of laser structures is

explained by the existence of a fairly well-developed theory [see, for example, 8]. According to the classical theory, the use of the dependence of the thermionic-emission current was allowed in calculating the rate of escape of electrons and holes from the QWs of laser heterostructures. The results of theoretical and experimental investigations of the temperature dependences of the threshold current density and the dependences of the time of carrier transport to the QW, time of carrier capture at the QW, and the rate of electron escape from the QW to the waveguide on the charge density in the QW are in good agreement [9–11]. In these studies, attention was focused on investigations of the laser efficiency in the regions of current densities in the subthreshold and near-threshold pumping modes, when electron escape plays a decisive role. Recognizing the indisputable validity of the dependence of the rate and time of electron and hole escape on the conduction-band discontinuity ΔE_c and valence-band discontinuity ΔE_v, we should note that there is no obvious interrelation of these dependences with the potential-barrier height and the space-charge potential distribution, which affect the efficiency of carrier injection in the modes of high and ultrahigh pump current densities.

The aim of this study is to investigate the features of carrier transport across the boundary of the active and waveguide regions, taking into account the effective potential-barrier height during the capture of electrons at QWs and escape of holes and electrons from QWs to the waveguide region, determine the scattering cross sections for excess carriers in the waveguide region, and establish the contributions of charge emission from QWs and internal optical loss to the current dependence of the optical efficiency using expanded-core waveguide lasers in the system of AlGaAs/GaAs/InGaAs solid solutions.

2. FUNDAMENTALS OF THE PHYSICAL MODEL

To describe the current dependence of the output optical power P_{out} of a laser, we used the classical formula that takes into account the efficiency of conversion of the fraction of recombining carriers into photons with the energy $h\nu$ for currents I higher than the threshold value I_{th}. In the stimulated-emission mode, the efficiency of conversion of the current into light is determined by the external differential quantum efficiency with regard to the internal optical loss α_i and the loss α_m to radiation extraction from a laser stripe cavity, as well as the internal differential quantum efficiency η_i:

$$\begin{aligned} P_{\text{out}} &= \eta_i(h\nu/q)[\alpha_m/(\alpha_m+\alpha_i)](I-I_{\text{th}}) \\ &= \eta_s^d\eta_r^d\eta_i^d(h\nu/q)[\alpha_m/(\alpha_m+\alpha_i)](I-I_{\text{th}}). \end{aligned} \quad (1)$$

In formula (1), η_i is presented by the product of three components, where η_s^d is the differential efficiency of injection within the geometric size of the laser stripe, η_r^d is the differential efficiency of radiative recombination, η_i^d is the differential efficiency of injection into the quantum-confined active region, and q is the electron charge. In the absence of current leakage during the pumping of laser structures and the saturation of nonradiative-recombination channels, the parameters η_s^d and η_r^s can be taken to be unity with high accuracy, while the parameter η_i^d demonstrates a pronounced dependence on the current.

To establish the functional current dependence $\eta_i^d = f(J)$ (J is the current density), we studied the features of the indirect injection of carriers into the SCDH active region, taking into account that the interfaces between the waveguide and active regions contain isotype N–n heterojunctions with the conduction-band discontinuity ΔE_c, valence-band discontinuity ΔE_v, and the potential distribution in the space-charge region, which determine the potential-barrier heights φ^{bp}, φ_1^{be}, and φ_2^{be} (Fig. 1). In the quasi-steady-state case, the current density at the interface between the QW and the waveguide on the N-emitter side is equal to the sum of the density J^e of the electron drift current and the density J_{esc}^p of the thermal escape of holes from the QW

$$J = J^e + J_{\text{esc}}^p. \quad (2)$$

Then, the current density at the interface between the QW and the waveguide on the emitter side is equal to the sum of the density J^p of the diffusion hole current and the density J_{esc}^e of the thermionic electron current

$$J = J^p + J_{\text{esc}}^e. \quad (3)$$

The density J^e of the drift current from the N-emitter side was calculated according to classical Schottky thermionic emission–diffusion theory [12], which is valid also for isotype heterojunctions

$$\begin{aligned} J^e &= qN_cV_D\exp(-q\varphi_1^{be}/kT) \\ &= qN_cV_D\exp[-(\Delta E_c - E_f^e/kT)]\exp(qU/kT). \end{aligned} \quad (4)$$

In (4), V_D and N_c are the drift velocity and density of states in the waveguide conduction band, k is the Boltzmann constant, U is the bias voltage at the N–n heterojunction, q is the electron charge, T is the temperature, and E_f^e is the Fermi-level position in the GaAs waveguide. In the Schottky approximation, the maximum field at the waveguide–QW interface reaches (3–7) × 10^3 V/cm in the case of linear field distribution in the space-charge region of isotype

N–n heterojunctions upon background doping in the range of (1–3) × 10^{16} cm^{-3}. This means that the drift velocity is $V_D \approx 2 \times 10^7$ cm/s, which is close to the maximum drift velocities in GaAs. The densities of the thermionic-emission currents from the QW were determined under the assumption of the above-barrier transport of carriers (electrons and holes) located in the first quantum-confinement subband with an energy of $\varepsilon^1_{e,p} = \pi^2\hbar^2/(2m^*_{e,p}d^2)$, where $m^*_{e,p}$ is the electron or hole effective mass in the QW, $\hbar$ is Planck's constant, and d is the QW thickness:

$$J^p_{\text{esc}} = (4\pi q m^*_p/h^3)(kT)^2 \exp[-(q\varphi^{bp}/kT)]$$
$$= (4\pi q m^*_p/h^3)(kT)^2 \exp[-(\Delta E_c + \Delta E_v - E^p_f)/kT] \times \exp(qU/kT), \quad (5)$$

$$J^e_{\text{esc}} = (4\pi q m^*_e/h^3)(kT)^2 \exp[-(q\varphi^{be}_2/kT)]$$
$$= (4\pi q m^*_e/h^3)(kT)^2 \exp[-(\Delta E_c - E^e_f)/kT]/kT. \quad (6)$$

SCDH lasers with a single quantum-confined active region made of $In_{0.3}Ga_{0.7}As$ solid solution with a thickness of $d = 100$ Å were examined. The energies calculated for the first quantum-confinement levels of electrons and holes are 26 and 11 meV. The effective masses of holes and electrons for the QW material are $m^*_p = 0.356m_0$ and $m^*_e = 0.063m_0$, respectively, where m_0 is the free electron mass. The calculated effective densities of states are $N^{2D}_c = 6.79 \times 10^{11}$ cm^2 for two-dimensional (2D) electrons in the QW conduction band and $P^{2D}_v = 3.84 \times 10^{12}$ cm^2 for 2D holes in the valence band. The structures contained an extended GaAs-based waveguide region with a total thickness of 1.5 μm. The SHDCs had asymmetrically arranged active regions to minimize the contribution of higher optical modes. The thickness of the waveguide region was $d_1 = 1.2$ μm from the N-type emitter side and $d_2 = 0.3$ μm from the P-type emitter side. In the calculation, the values of $\Delta E_c = 182$ meV and $\Delta E_v = 113$ meV were used. The laser had a stripe width of 100 μm with a Fabry–Perot cavity length of ~3 mm. The loss to radiation extraction from the laser stripe cavity was taken to be $\alpha_m = 5.1$.

The current dependences of the time of thermionic emission from the quantum-confined active region of the laser to the waveguide are calculated.

Under quasi-neutrality conditions at equal excess carrier densities in the QW ($N^{QW} = P^{QW}$), the current dependences of the electron and hole escape times $\tau^e_{\text{esc}} = qdN^{QW}/J^e_{\text{esc}}$ and $\tau^p_{\text{esc}} = qdP^{QW}/J^p_{\text{esc}}$ are fundamentally different (Fig. 2). Here, in the numerical simulation, we used linear approximation of the dependence of the carrier density in the QW on the pump current $N^{QW} = P^{QW} = J^p\tau_{\text{ph}}$. The photon lifetime τ_{ph} in the laser cavity was calculated as $\tau_{\text{ph}} = 1/\alpha_m v_{\text{gr}} = \bar{n}/\alpha_m c$, where v_{gr} and c are the photon group velocity and the speed of light, respectively. The refractive index of the GaAs waveguide is $\bar{n} = 3.45$. Next, we estimate the internal optical loss α_i of the laser power and, where necessary, make corrections in the numerical simulation of the current dependence of the coefficient of injection into the QW.

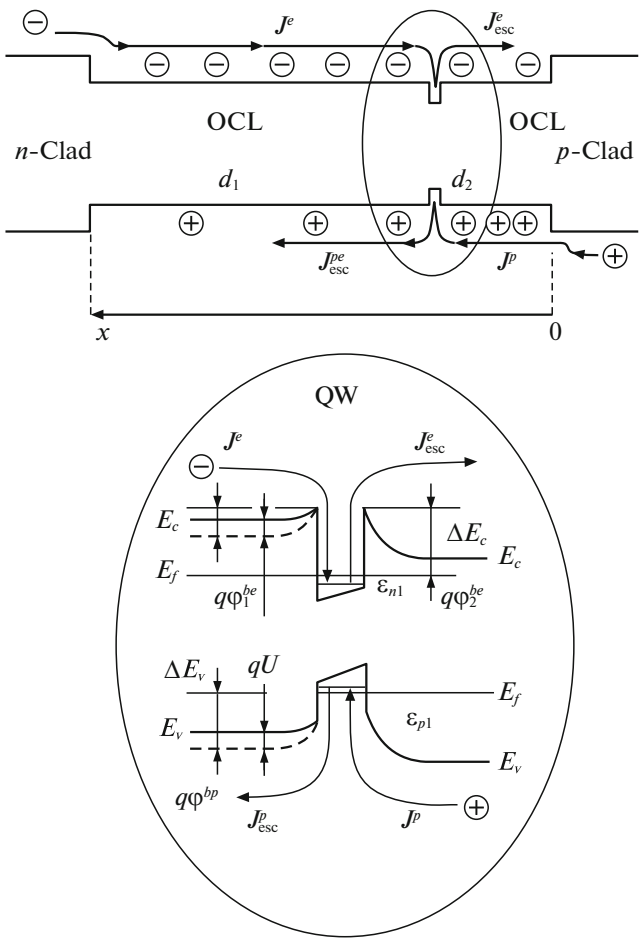

Fig. 1. Band energy diagram at the interfaces between the active and waveguide regions of an injection pulsed laser with an asymmetric waveguide.

3. USING THE DRUDE–LORENTZ DISPERSION RELATIONS TO ESTIMATE THE SCATTERING CROSS SECTIONS IN THE GaAs WAVEGUIDE

Representing a substance as a set of harmonic oscillators in the Drude–Lorentz theory to describe the response of a medium to electromagnetic radiation (EMR), one can determine a fraction of the emission power loss during EMR propagation in a conducting medium. We use the fundamentals of the dispersion model for semiconductors [see, for example, 13, 14] to estimate the internal optical loss in the investigated

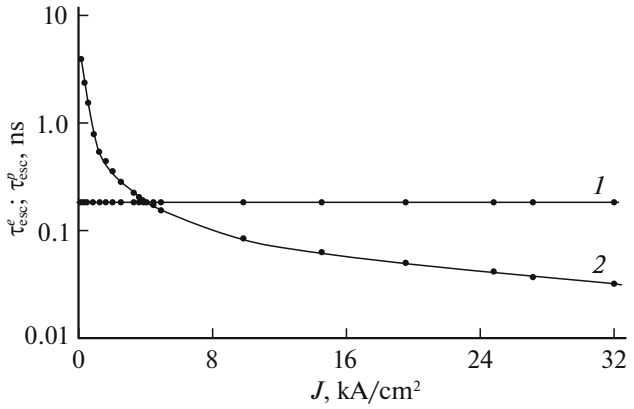

Fig. 2. Current dependences of the thermionic-emission time for electrons (curve *1*) and holes (curve *2*) from the quantum-confined active region of the laser to the waveguide.

laser structures. For the harmonic EMR field with the frequency ω, any processes that cause the absorption of radiation energy lead to the occurrence of the imaginary component of the permittivity

$$\varepsilon'' = Nq^2/m^*_{e,p}\varepsilon_0\omega\tau/(1+\omega^2\tau^2). \quad (7)$$

Here, $m^*_{e,p}$ is the effective mass of free carriers (electrons or holes) in the GaAs waveguide, N and q are the density and value of the excess carrier charge, and τ is the carrier momentum-relaxation time, which, in the case of energy independence, is related to the mobility μ and effective mass m^* as $\tau = (m^*\mu)/q$.

Since the excess carrier distribution in the waveguide of a laser structure is described by the ambipolar diffusion (drift) coefficient, the momentum-relaxation time was calculated using the ambipolar mobility. For the waveguide with *n*-type conductivity at typical background impurity levels of ~10^{16} cm^{-3}, the ambipolar mobility was determined by the hole mobility and, with an increase in the current, its value changed from $\mu_p = 300$ cm^2/(V s) to $2b/(b+1)\mu_p = 570$ cm^2/(V s). The momentum-relaxation time was considered to be a measure of the inertia of a single electron-hole ensemble, which takes into account the response of a substance to the EMR for any coordinate of the injected carrier density distributed over the waveguide region ($N \sim p$, n). Under quasi-neutrality conditions, the excess electron and hole momentum relaxation was described by equal times with the corresponding values of $\tau = (m^*_p\mu)/q$. Simultaneously, the difference between the frequencies of the longitudinal plasma oscillations of electrons and holes was taken into account in the calculation of dielectric function (7) at any N values corresponding to the laser pump-current density.

The imaginary part of the complex permittivity calculated using formula (7) allows us to estimate the absorption index k and the absorption coefficient α using the classical relations $\varepsilon'' = 2\bar{n}k$ and $\alpha = 4\pi k/\lambda$. Here, n is the refractive index of the waveguide material and λ is the emission wavelength. Writing the functional dependence of the absorption coefficient on the free carrier density in the form $\alpha_{e,p} = \sigma_{e,p}N$, we estimate the scattering cross sections σ_e, p for electrons and holes, respectively. It was found that, for high-power pulsed lasers with $\lambda = 1.06$ μm ($\omega = 1.78 \times 10^{15}$ s^{-1}), the scattering cross sections are $\sigma_e = 1.05 \times 10^{-18}$ cm^2 and $\sigma_p = 1.55 \times 10^{-19}$ cm^2. The obtained values agree well with the data from [15], where the numerical values of the coefficients of absorption at free carriers for different semiconductors, including *III–V* ones, and their dependence on the electron density were reported. Below, the obtained scattering cross sections are used to calculate the current dependences of the absorption coefficient and estimate the internal optical loss in the waveguide at different pump-current levels.

4. DETERMINING THE RELATIVE CONTRIBUTION OF THE ESCAPE RATE AND INTERNAL OPTICAL LOSS TO THE SATURATION OF THE *P–I* CHARACTERISTIC OF HIGH-POWER PULSED LASERS

In the numerical analysis of the *P–I* characteristics of the injection laser, we used a system of rate equations describing the processes of an increase and a decrease in the carrier density in the QW. In these equations, the density increment is determined by the injection current and the density decrement, by the spontaneous and stimulated recombination rate and the thermionic emission of electrons and holes from the QW to the waveguide. In addition to the total number N^{QW} (P^{QW}) of carriers in the active region, the total number of photons S in the cavity was used. The rate of variation in the number of photons dS/dt was controlled by an increase in their number under stimulated emission $v_{gr}GS$ and a decrease in it caused by optical loss in the cavity. When considering the number of photons in the cavity, only the photons created by the stimulated-emission events were taken into account, while spontaneous emission was ignored. Under this assumption, we have $S \approx N^{QW} - P^{QW}$ and the error of further estimation is no higher than $\tau_{ph}/\tau_d \approx 10^{-2}$, where τ_d is the differential carrier lifetime in the QW. The rate of a decrease in the photon density in the cavity was specified via the photon lifetime τ_{ph}. Thus, the system of rate equations had the form

$$\begin{aligned} dP^{QW}/dt &= J^p/q - J^p(\tau_{ph}/\tau^p_{esc})/q - S/\tau_{ph} \\ &= J^p/q - J^p_{esc}/q - S/\tau_{ph}, \end{aligned} \quad (8)$$

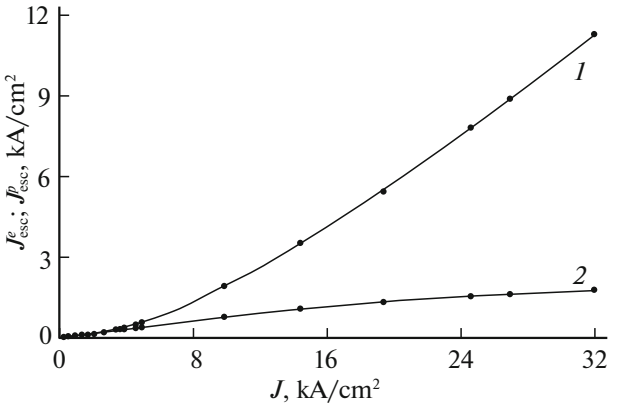

Fig. 3. Dependences of the density of the thermionic-emission currents of holes J^p_{esc} (curve *1*) and electrons J^e_{esc} (curve *2*) on the pulsed pump-current density J.

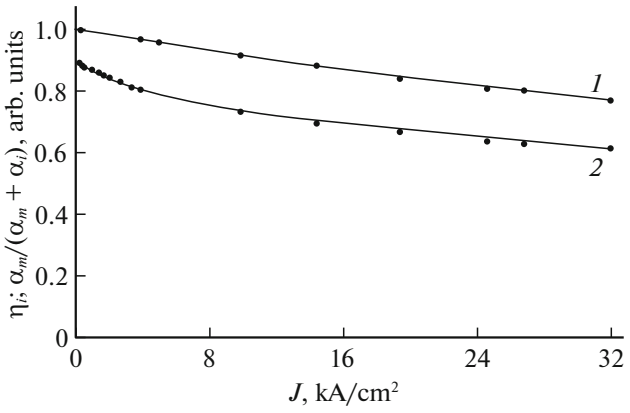

Fig. 4. Current dependences of the relative fraction of loss to radiation extraction in the sum of loss to radiation extraction from the laser cavity and free carrier absorption $\alpha_m/(\alpha_m + \alpha_i)$ (curve *1*) and differential injection efficiency (curve *2*).

$$dN^{QW}/dt = J^e/q - J^e(\tau_{ph}/\tau^e_{esc})/q - S/\tau_{ph} = J^e/q - J^e_{esc}/q - S/\tau_{ph}. \quad (9)$$

Using the system of equations (8) and (9) for the quasi-steady states $dP^{QW}/dt = dN^{QW}/dt = 0$ (taking into account the equality $P^{QW} = N^{QW}$), we determined the current dependences of J^p_{esc} and J^e_{esc} (Fig. 3), as well as the current dependence of the differential injection efficiency $\eta^d_i = f(J) = (J - J^p_{esc} - J^e_{esc})/J$ (curve *2*, Fig. 4) into the QW. Figure 3 shows the calculated dependences of the hole thermionic current density J^p_{esc} (curve *1*) and the electron thermionic current density J^e_{esc} (curve *2*) on the pulsed laser pump-current density. It was established that in SCDH-based lasers in the system of AlGaAs/GaAs/InGaAs solid solutions with $\lambda = 1.06$ μm in the pump-current density range of $J_{th} \le J \le 30J_{th}$, the electron thermionic-emission current exceeds the hole thermionic-emission current and, at $J_{th} \le J \le 8J_{th}$, the ratio between the thermionic-emission currents is $J^e_{esc}/J^p_{esc} \ge 5$. In the region of high and ultrahigh injection levels, the hole component of the thermionic-emission current significantly exceeds the electron component and, at a pump-current density of $J = 32$ kA/cm^2, their ratio reaches $J^p_{esc}/J^e_{esc} \ge 6$. The current dependences of J^e_{esc} and J^p_{esc} shown in Fig. 3 are consistent with the current dependences of the electron and hole emission times (Fig. 2) and confirm the presence of a pronounced feature in filling the QWs with excess carriers. Holes freely come into the QW via diffusion, while for electrons to overcome the potential barrier at the interface, according to (4), a fixed positive-bias level is required. As the current density increases, the positive-bias level on the isotype N–n junction grows, which leads to a decrease in the potential barrier for holes and an increase in the hole thermionic-emission current from the QW to the waveguide in accordance with (5). Simultaneously with current growth, the two-dimensional electron density N^{QW} in the QW increases, which leads to a shift of the quasi-Fermi level and a decrease in the potential barrier φ^{be}. As a result, the electron thermionic-emission current density increases in accordance with dependence (6). Equations (4)–(6) for the current densities show the presence of both regularities that are common with the classical theory [12] and the differences characteristic of a two-dimensional system. Thus, the current components J^e and J^p_{esc}, which depend on the corresponding potential-barrier heights φ^{be}_1 and φ^{bp}, have a pronounced I–V characteristic $J^e \propto \exp(qU/kT)$ and $J^p_{esc} \propto \exp(qU/kT)$, while the current component J^e_{esc} only depends on the degree of electron filling of the first quantum-confinement level of the active region and is determined by the potential-barrier height φ^{be}_2 (Fig. 1). The presence of the exponential component in the I–V characteristic of the hole thermionic-emission current explains its superlinear dependence on the laser pump-current density.

In the numerical analysis of the P–I characteristics of the injection laser, we took into account the current dependence of the internal optical loss $\alpha_i = f(J)$ of the laser radiation power, which is determined by the radiation-scattering cross section and the excess carrier density in the waveguide $\alpha_{e,p} = \sigma_{e,p}N$. To determine the excess carrier density distribution ($N \sim p, n$), a one-dimensional system of equations was solved for an arbitrary injection level in the waveguide on both sides of the QW. The initial system of equations for the currents has the form

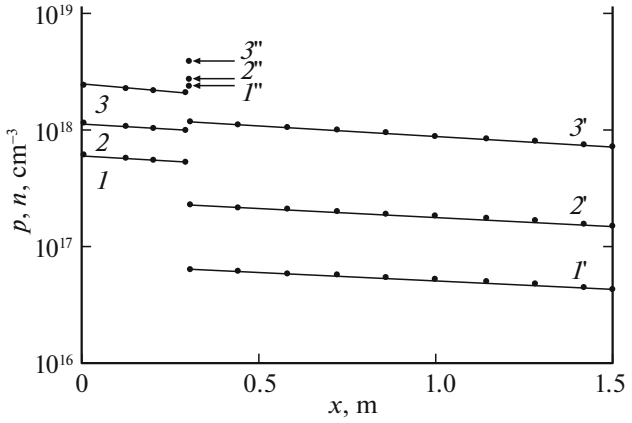

Fig. 5. Excess carrier density distribution (p, n) in the waveguide on the P-type emitter side (*1*, *2*, *3*), in the waveguide on the N-type emitter side (*1'*, *2'*, *3'*), and in the quantum-confined active region (*1"*, *2"*, and *3"*) of the laser at pulsed pump-current amplitudes J of (*1*, *1'*, *1"*) 14, (*2*, *2'*, *2"*) 30, and (*3*, *3'*, and *3"*) 100 A.

$$J = qpE\mu_p - qD_p dp/dx \tag{10}$$

with the boundary condition

$$x = 0, \quad p = JL_p/qD_p,$$

$$J^p_{\text{esc}} = qpE\mu_p - qD_p dp/dx \tag{11}$$

with the boundary condition

$$x = 0.3, \quad p = J^p_{\text{esc}} L_p/qD_p,$$

$$J^e = qE\mu_e n. \tag{12}$$

The problem was solved under the following assumptions:

—the nonradiative lifetime and mobility of the majority carriers (electrons) are independent of the injection level: τ_e and μ_e;

—the excess minority carrier lifetime τ_p was calculated as a function of the injection level as $1/\tau_p = 1/(A + Bp)$, where $A = 10^8$ s^{-1} is the coefficient of nonradiative monomolecular recombination through local centers and $B = 10^{-10}$ cm^3 s^{-1} is the radiative-recombination coefficient;

—the electron component of the current in the waveguide region on the N-type emitter side ensures the preservation of quasi-neutrality in the waveguide and the QW and corresponds to the rate of recombination of injected minority carriers.

Excluding the electric-field strength from Eqs. (10) and (11) and using the current dependences of the drift velocity $v_p = \mu_p E = (1/q)J/[(b + 1)p + bn^0]$ from [16] and the ambipolar diffusivity $D_p = (2p + n^0)/[(b + 1)p + bn^0]bD_p$, we managed to calculate the excess carrier distribution in the waveguide (Fig. 5). It can be seen that the density level in the waveguide on the P-type emitter side substantially exceeds the background doping concentration and attains $p(n) > 10^{18}$ cm^{-3} at a pump-current density of $J \geq 10$ kA/cm^2. In the waveguide on the N-type emitter side, the excess carrier density profile is determined by the hole thermionic-emission current from the QW. Already at pump currents of $J \approx 5 \times 10^3$ kA/cm^2, the density level $p(n)$ in this waveguide region exceeds the background doping level, which affects the condition of radiation propagation in the laser cavity.

Taking into account the asymmetric position of the QW in the waveguide, we calculated the fraction of the internal optical loss

$$\alpha_i = \sum_{x=0}^{x=0.3} 0.2\langle\sigma_e n(x) + \sigma_p p(x)\rangle + \sum_{x=0.3}^{x=1.5} 0.8\langle\sigma_e n(x) + \sigma_p p(x)\rangle.$$

Since in the lasers with wide waveguides the waveguide optical limiting factor for the main mode reaches 0.99, the internal optical loss to the mobile majority carriers in the P- and N-type emitters were taken to be zero. Figure 4 shows the current dependence of the relative fraction of loss to radiation extraction in the sum of the loss to radiation extraction from the laser cavity and absorption at free carriers $\alpha_m/(\alpha_m + \alpha_i)$ (curve *1*). It was established that the internal optical loss determined by the density level of excess carriers injected by the hole thermionic-emission currents makes a significant fraction of the total optical loss in the waveguide. In particular, for a pump-current density of $J = 32$ kA/cm^2, the fraction of internal optical loss was $\alpha_i = 0.55$ cm^{-1} in the waveguide on the P-type emitter side and $\alpha_i = 0.93$ cm^{-1} in the waveguide on the N-type emitter side.

In calculating the laser I–V characteristics, we used classical formula (1) and the calculated current dependences of the differential efficiency η_i^d of injection into the QW and the relative fraction of loss to radiation extraction in the sum of loss to radiation extraction from the laser cavity and absorption at free carriers $\alpha_m/(\alpha_m + \alpha_i)$ (Fig. 4). In Fig. 6, to illustrate the role of the internal optical and injection loss, the curves are shown for zero loss (curve *1*), with regard to the internal optical loss ($\alpha_i > 0$ and $\eta_i^d = 1$) (curve *2*), and with regard to the internal optical and current injection loss ($\alpha_i > 0$ and $\eta_i^d < 1$) (curve *3*). Curve *3* has a pronounced sublinear shape, which corresponds to the experimental P–I characteristics [1–3, 6, 7, 17, 18]. For the SCDH-based lasers in the AlGaAs/GaAs/InGaAs solid-solution system, it was found that the internal optical loss makes up a small fraction of the loss and saturation of the P–I characteristic and the sublinear current dependence of the

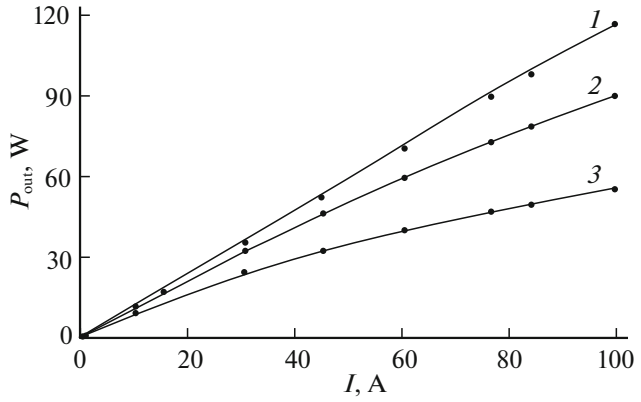

Fig. 6. Calculated dependences of the P–I characteristic of a SCDH-based laser in a system of AlGaAs/GaAs/InGaAs solid solutions (*1*) in the absence of internal optical and current injection loss ($\alpha_i = 0$ and $\eta_i^d = 1$), (*2*) with regard to the internal optical loss ($\alpha_i > 0$ and $\eta_i^d = 1$), and (*3*) with regard to the internal optical and current injection loss ($\alpha_i > 0$ and $\eta_i^d < 1$).

injection coefficient are related to an increase in the rate of hole escape to the waveguide.

5. CONCLUSIONS

The results of investigations of the current dependence of the efficiency of injection into the QWs of SCHD-based lasers were presented. A physical model that takes into account the feature of carrier transport through the interface between the active and waveguide regions was proposed. The fraction of the thermionic currents of electrons and holes in a wide range of pump-current densities, from near-threshold to ultrahigh (>10 kA/cm^2), was estimated. It was shown that, at pump-current densities close to the threshold values, the electron emission has a decisive effect on the efficiency of the injection of carriers into the QW, which is consistent with the conclusions made in [9–11]. With an increase in the injection level as a result of a decrease in the potential-barrier effective height, the fraction of the hole thermionic current substantially increases. At a pump-current density of J = 32 kA/cm^2, the hole thermionic-current density reaches $J_{esc}^p \approx 11$ kA/cm^2 and the electron thermionic-emission density reaches $J_{esc}^e \approx 1.8$ kA/cm^2.

To estimate the fraction of the internal optical loss and analyze the conditions for the propagation of laser radiation in the waveguide, we used the calculated relations between the electrodynamic and optical properties of the laser heterostructure. The scattering cross sections for excess carriers in a GaAs waveguide were obtained. For the high-power pulsed lasers with $\lambda = 1.06$ μm, we found $\sigma_e = 1.05 \times 10^{-18}$ cm^2 and $\sigma_p = 1.55 \times 10^{-19}$ cm^2. These scattering cross sections significantly differ from the values used, for example, in [1, 17, 18] for estimating the internal optical loss, but agree well with the data from [15].

The results of numerical simulation and the analysis performed allowed us to estimate the relative contribution of two main mechanisms: free carrier absorption and spontaneous recombination in the waveguide regions due to the escape of carriers from the QW. Good agreement was obtained between the calculated and experimental P–I characteristics [17, 18] of SCHD-based lasers in the AlGaAs/GaAs/InGaAs solid-solution system. It was established that the internal optical loss makes a small fraction of the loss and the saturation of the P–I characteristic and the sublinear current dependence of the injection coefficient are related to an increase in the rate of hole escape into the waveguide. Thus, the prospect for enhancing the power of pulsed semiconductor lasers is related, to a great extent, to the possibility of suppressing the delocalization of carriers from QWs, which makes it relevant to use asymmetric heterostructures [19] or their alternatives, i.e., simulated doped SCDHs. Further experimental investigations should confirm the validity of the conclusions made.

ACKNOWLEDGMENTS

I thank N.S. Averkiev and K.V. Reikh for consultations and useful discussions on the current emission of carriers in two- and three-dimensional electronic structures.

CONFLICT OF INTEREST

The author declares that he has no conflict of interest.

REFERENCES

1. Z. N. Sokolova, D. A. Veselov, N. A. Pikhtin, I. S. Tarasov, and L. V. Asryan, Semiconductors **51**, 959 (2017).
2. H. Wenzel, P. Crump, A. Pietrzak, C. Roder, X. Wang, and G. Erbert, Opt. Quant. Electron. **41**, 645 (2009).
3. X. Wang, P. Crump, H. Wenzel, A. Liero, T. Hoffmann, A. Pietrzak, C. M. Schultz, A. Klehr, A. Ginolas, S. Einfeldt, F. Bugge, G. Erbert, and G. Trankle, IEEE J. Quant. Electron. **46**, 658 (2010).
4. E. A. Avrytin and B. S. Ryvkin, Semicond. Sci. Technol. **32**, 1 (2017).
5. L. W. Hallman, B. S. Ryvkin, E. A. Avrytin, A. T. Aho, J. Viheriala, M. Guina, and J. T. Kostamovaara, IEEE Photon. Tecnol. Lett. **31**, 1635 (2019).
6. J. Piprek and Z.-M. Li, IEEE Photon. Technol. Lett. **30**, 963 (2018).
7. J. Piprek, Opt. Quant. Electron. **51**, 60 (2019).
8. N. Tansu and L. J. Mawst, J. Appl. Phys. **97**, 054502 (2005).

9. I. S. Shashkin, D. A. Vinokurov, A. V. Lyutetskiy, D. N. Nikolaev, N. A. Pikhtin, N. A. Rudova, Z. N. Sokolova, S. O. Slipchenko, A. L. Stankevich, V. V. Shamakhov, D. A. Veselov, K. V. Bakhvalov, and I. S. Tarasov, Phys. Semicond. Dev. **46**, 1211 (2012).

10. S. O. Slipchenko, I. S. Shashkin, L. S. Vavilova, D. A. Vinokurov, A. V. Lyutetskiy, N. A. Pikhtin, A. A. Podoskin, A. L. Stankevich, N. V. Fitisova, and I. S. Tarasov, Semiconductors **44**, 661 (2010).

11. A. E. Zhukov, N. V. Kryzhanovskaya, F. I. Zubov, Y. M. Shemyakov, M. V. Maximov, E. S. Semenova, Kr. Yvind, and L. V. Asryan, Appl. Phys. Lett. **100**, 021107 (2012).

12. S. M. Sze, *Physics of Semiconductor Devices* (Wiley, New York, 1981), Vol. 1.

13. V. B. Timofeev, *Optical Spectroscopy of Bulk Semiconductors and Nanostructures* (Lan', St. Petersburg, 2015), Chap. 16, p. 136 [in Russian].

14. D. I. Belenko, *Complex Dielectric Constant. Plasma Resonance of Free Charge Carriers in Semiconductors* (Sarat. Univ., Saratov, 1999), p. 8 [in Russian].

15. H. Y. Fan, Semicond. Semimet. **3**, 405 (1967).

16. Zh. I. Alferov, V. I. Korol'kov, I. M. Konicheva, V. S. Yuferev, and A. A. Yakovenko, Sov. Phys. Semicond. **13**, 157 (1979).

17. D. A. Veselov, V. A. Kapitonov, N. A. Pikhtin, A. V. Lyutetskii, D. N. Nikolaev, S. O. Slipchenko, Z. N. Sokolova, V. V. Shamakhov, I. S. Shashkin, and I. S. Tarasov, Quantum Electron. **44**, 993 (2014).

18. D. A. Veselov, N. A. Pikhtin, A. V. Lyutetskii, D. N. Nikolaev, S. O. Slipchenko, Z. N. Sokolova, V. V. Shamakhov, I. S. Shashkin, and I. S. Tarasov, Quantum Electron. **45**, 604 (2015).

19. F. I. Zubov, A. E. Zhukov, Yu. M. Shernyakov, M. V. Maximov, N. V. Kryzhanovskaya, K. Yvind, E. S. Semenova, and L. V. Asryan, Tech. Phys. Lett. **41**, 439 (2015).

Translated by E. Bondareva